

## The $2^+$ excitation of the Hoyle state

Dao T. Khoa<sup>1</sup>, Do Cong Cuong<sup>1</sup>, and Yoshiko Kanada-En'yo<sup>2</sup>

<sup>1</sup>Institute for Nuclear Science and Technology, Vinatom, 179 Hoang Quoc Viet, Hanoi, Vietnam

<sup>2</sup>Department of Physics, Kyoto University, Kyoto 606-8502, Japan

**Abstract.** To understand why the  $2^+$  excitation of the Hoyle state was so difficult to observe in the direct reaction experiments with the  $^{12}\text{C}$  target, a detailed folding model + coupled-channel analysis of the inelastic  $\alpha+^{12}\text{C}$  scattering at  $E_{\text{lab}} = 240$  and  $386$  MeV has been done using the complex optical potential and inelastic scattering form factor obtained from the double-folding model using the nuclear transition densities predicted by the antisymmetrized molecular dynamics. With the complex strength of the density dependent nucleon-nucleon interaction fixed by the optical model description of the elastic  $\alpha+^{12}\text{C}$  scattering, the inelastic scattering form factor was fine tuned to the best coupled-channel description of the  $(\alpha, \alpha')$  cross section measured for each excited state of  $^{12}\text{C}$ , and the corresponding isoscalar  $E\lambda$  transition strength has been accurately determined. The present analysis of the  $(\alpha, \alpha')$  data measured in the energy bins around  $E_x \approx 10$  MeV has unambiguously revealed the  $E2$  transition strength that should be assigned to the  $2_2^+$  state of  $^{12}\text{C}$ . A very weak transition strength  $B(E2; 0_1^+ \rightarrow 2_2^+) \approx 3 e^2\text{fm}^4$  has been established, which is smaller than the  $E2$  strength predicted for the transition from the Hoyle state to the  $2_2^+$  state by at least two orders of magnitude. This is one of the main reasons why the direct excitation of the  $2_2^+$  state of  $^{12}\text{C}$  has been difficult to observe in the experiments.

The synthesis of  $^{12}\text{C}$  during the helium burning process is known to proceed through the triple- $\alpha$  reaction, where an unstable  $^8\text{Be}$  formed by the fusion of two  $\alpha$ -particles captures the third  $\alpha$ -particle to form  $^{12}\text{C}$  in the  $0^+$  excited state at  $7.65$  MeV, which decays to the ground state via  $\gamma$  emission. This monopole excitation of  $^{12}\text{C}$  (named as Hoyle state) has been first predicted by Fred Hoyle [1] in 1953, and observed later in the deuteron pickup reaction  $^{14}\text{N}(d, \alpha)^{12}\text{C}^*(E_x = 7.653 \text{ MeV})$  [2]. The Hoyle state resonantly boosts the triple- $\alpha$  reaction rate by a factor up to  $10^8$  [3], which is needed to account for the carbon abundance in nature. Besides its unique role in the carbon synthesis, the Hoyle state is also famous as having a pronounced three  $\alpha$ -cluster structure. Given a nonspherical shape of the  $^8\text{Be} + \alpha$  configuration, an excited rotational band with the angular momentum  $J^\pi = 2^+, 4^+, \dots$  built upon the Hoyle state was suggested long ago by Morinaga [4]. The second  $2^+$  state of  $^{12}\text{C}$  was also predicted by the different structure models like the Resonating Group Method [5, 6] or the antisymmetrized molecular dynamics (AMD) [7, 8] at the excitation energy around  $10$  MeV, about  $2$  MeV above the  $\alpha$  threshold. Because of the pronounced  $\alpha$ -cluster structure predicted for the  $2_2^+$  state of  $^{12}\text{C}$ , many experimental studies were aimed to observe it in the spectra of the different reactions involving  $^{12}\text{C}$  (see the recent review [3]). The observation of the  $2_2^+$  state of  $^{12}\text{C}$  is important for a deeper understanding of the structure of the Hoyle state (to determine, e.g., the moment of inertia and deformation of  $^{12}\text{C}$  being in the Hoyle state [4, 9]). Although some evidence for a broad  $2^+$  resonance

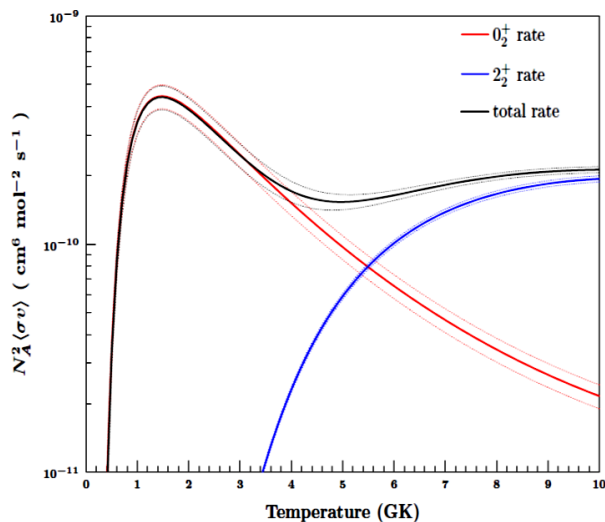


**Figure 1.** (Color online) Triple- $\alpha$  reaction rate estimated with or without the contribution from the  $2_2^+$  state of  $^{12}\text{C}$ . The illustration is taken from Ref. [12].

was found in several experiments that might be assigned to the  $2_2^+$  state of  $^{12}\text{C}$ , the clear identification of this state could only be made recently in the high-precision  $(\alpha, \alpha')$  experiment at  $E_\alpha = 386$  MeV [10] and  $\gamma$ -induced breakup  $^{12}\text{C}(\gamma, \alpha)^8\text{Be}$  reaction [11, 12].

The structure information about the excitation energy and  $E2$  transition strength of the  $2_2^+$  state of  $^{12}\text{C}$  is also

important for the determination the reaction rate of the triple- $\alpha$  process. For example, Zimmerman has shown [12] that taking into account the  $2_2^+$  state substantially enhances the triple- $\alpha$  reaction rate at the high temperatures of 5 to 10 GK (see Fig. 1). Given a very strong  $E2$  transition between the Hoyle state and  $2_2^+$  state predicted by the AMD calculation [13], the two-step process  ${}^8\text{Be} + \alpha \rightarrow {}^{12}\text{C}^*(2_2^+) \rightarrow {}^{12}\text{C}^*(0_2^+) \rightarrow {}^{12}\text{C}(0_1^+)$  should dominate the triple- $\alpha$  process at these high temperatures.

The AMD was proven to deliver a realistic description of the  $\alpha$ -cluster states in the light nuclei, and the AMD results for the excitation energies and  $E\lambda$  transition strengths of the excited  $2_1^+$ ,  $0_2^+$ , and  $3_1^-$  states of  ${}^{12}\text{C}$  agree reasonably with the experimental data [13]. At variance with the shell-model like  $2_1^+$  state, the  $2_2^+$  state was shown to have a well defined cluster structure (see Fig. 5 of Ref. [7]). It is remarkable that the predicted  $E2$  transitions from the Hoyle state to the  $2_2^+$  state and from the  $2_2^+$  state to the  $4_2^+$  state,  $B(E2; 0_2^+ \rightarrow 2_2^+) \approx 511 e^2\text{fm}^4$  and  $B(E2; 2_2^+ \rightarrow 4_2^+) \approx 1071 e^2\text{fm}^4$ , are much stronger than the  $E2$  transitions between the members of the ground-state band,  $B(E2; 0_1^+ \rightarrow 2_1^+) \approx 42.5 e^2\text{fm}^4$  and  $B(E2; 2_1^+ \rightarrow 4_1^+) \approx 28.5 e^2\text{fm}^4$ . Thus, the  $E2$  transition rates predicted by the AMD strongly suggest that the  $2_2^+$  and  $4_2^+$  states are the members of a rotational band built upon the Hoyle state. The predicted direct excitation of the  $2_2^+$  state from the ground state is very weak,  $B(E2; 0_1^+ \rightarrow 2_2^+) \approx 2 e^2\text{fm}^4$ . That's the reason why it was so difficult to observe this state in the inelastic hadron scattering. Although a strong  $E2$  transition has been predicted for the excitation of the  $2_2^+$  state from the Hoyle state, the two-step excitation of  ${}^{12}\text{C}$  via the Hoyle state seems suppressed in the  $(\alpha, \alpha')$  scattering at medium energies as well as by the disintegration of the excited  ${}^{12}\text{C}^*$  into three  $\alpha$  particles. Moreover, there is always a strong population of the narrow  $3_1^-$  state at 9.64 MeV and broad  $0_3^+$  resonance at 10.3 MeV that hinders the  $2_2^+$  peak at about 10 MeV in the excitation spectrum of  ${}^{12}\text{C}$ . These are the main reason for the scarcity of the experimental observation of the  $2_2^+$  state.

The strong  $E\lambda$  transitions between the  $2_2^+$  state and other cluster states of  ${}^{12}\text{C}$  predicted by the AMD calculation [13] naturally imply that the coupled channel (CC) effects in the inelastic  $\alpha+{}^{12}\text{C}$  scattering should be significant. In the  $(\alpha, \alpha')$  experiments at  $E_\alpha = 240$  [14] and 386 MeV [10] with the  ${}^{12}\text{C}$  target, the  $(\alpha, \alpha')$  cross sections were measured accurately in small energy bins over a wide range of scattering angles and excitation energies. These data have been subjected to the multipole decomposition analysis (MDA) to disentangle contribution of different  $E\lambda$  multiplicities to the excitation of  ${}^{12}\text{C}$  in each energy bin. The MDA, based on the DWBA, consistently gave a much weaker  $E0$  transition strength of the Hoyle state, with  $M(E0; 0_1^+ \rightarrow 0_2^+) \approx 3.6 \sim 3.8 e \text{fm}^2$  [14] that is about 30% weaker than the experimental value  $M(E0)_{\text{exp}} \approx 5.4 e \text{fm}^2$  deduced from the  $(e, e')$  data [15]. The folding model + DWBA analysis of the same  $(\alpha, \alpha')$  data using the AMD transition density for the Hoyle state also gives the best-fit  $M(E0) \approx 3.65 e \text{fm}^2$  [13]. The CC effects were anticipated as the main reason for the missing monopole strength of

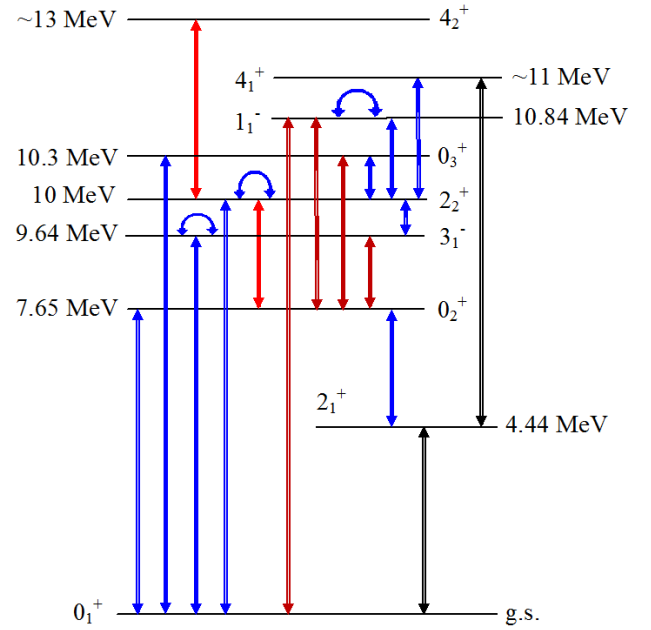


**Figure 2.** (Color online) Coupling scheme used in the Folding + CC analysis of the inelastic  $\alpha+{}^{12}\text{C}$  scattering data measured at  $E_\alpha = 240$  [14] and 386 MeV [10].

the Hoyle state observed in the DWBA analysis of the  $(\alpha, \alpha')$  scattering [16]. The original MDA of the 240 MeV data [14] could not identify the  $2_2^+$  peak in the  $(\alpha, \alpha')$  spectrum, while the MDA of the 386 MeV data [10] has disentangled the weak  $2_2^+$  peak and deduced the corresponding transition rate  $B(E2 \uparrow) \approx 2 e^2\text{fm}^4$ .

It is clear from the above discussion that one needs to carry out a comprehensive CC analysis of the  $(\alpha, \alpha')$  data for the determination of the transition strengths of the cluster states of  ${}^{12}\text{C}$ . In the present work, the coupling between all strong  $E\lambda$  transitions from the Hoyle and  $2_2^+$  states to the neighboring excited states of  ${}^{12}\text{C}$  were taken into account as shown in Fig. 2. The generalized folding model of Ref. [17] was used to evaluate the complex optical potential (OP) and inelastic scattering form factor (FF) from the (complex) effective nucleon-nucleon (NN) interaction between the projectile nucleon  $i$  and target nucleon  $j$  as

$$U_{A \rightarrow A^*} = \sum_{i \in \alpha; j \in A, j' \in A^*} [\langle ij' | v_D | ij \rangle + \langle ij' | v_{EX} | ji \rangle], \quad (1)$$

where  $A$  and  $A^*$  denote the target in the entrance- and exit channel of the  $(\alpha, \alpha')$  scattering, respectively. The direct ( $v_D$ ) and exchange ( $v_{EX}$ ) parts of the density dependent CDM3Y6 interaction [18] were used with the imaginary part determined [19] from the JLM complex nucleon OP in the nuclear matter [20]. Equation (1) gives the OP if  $A^* = A$  and inelastic scattering FF if otherwise. The AMD nuclear transition densities were used in the folding calculation (1). All the CC calculations were done with the complex folded OP and FF, using the code ECIS97 [21]. Because the exit channel contains  ${}^{12}\text{C}^*$  being in an excited state that is generally more dilute, the OP of each

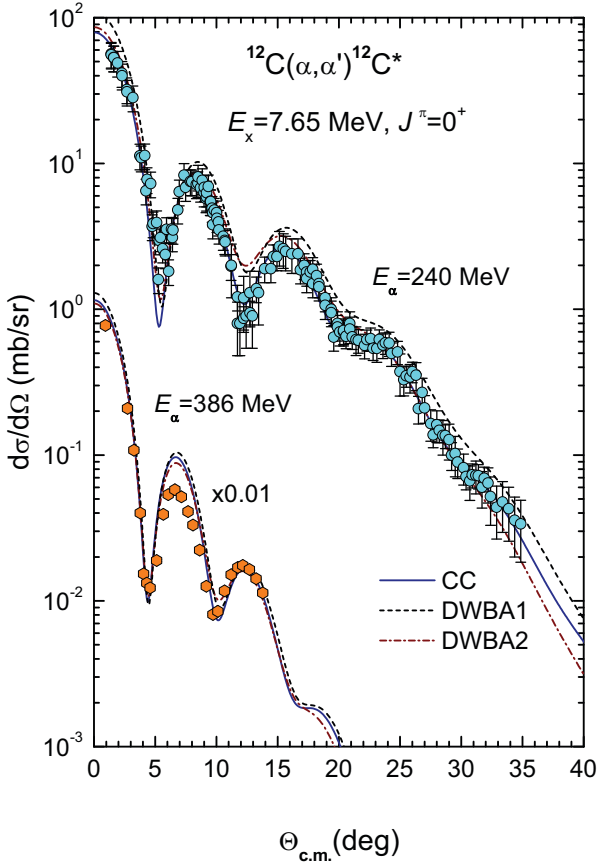


**Figure 3.** (Color online) DWBA and CC descriptions of the  $(\alpha, \alpha')$  data for the Hoyle state, measured at  $E_\alpha = 240$  MeV [14] and 386 MeV [10]. The DWBA1 results were obtained using the same OP for both the entrance and exit channels, and the DWBA2 and CC results were obtained with the OP of the exit channel computed separately at the energy  $E_\alpha - Q$ , using the AMD diagonal density of  $^{12}\text{C}^*(0_2^+)$ .

exit channel ( $U_{A^* \rightarrow A^*}$ ) has been computed separately using the diagonal ( $\lambda = 0$ ) density of  $^{12}\text{C}^*$  given by the AMD [7]. Such a treatment of the exit OP lead to a better agreement of the calculated cross sections with the data and helped to deduce accurately the  $B(E\lambda)$  values for the excited states under study [13].

The results of the folding model + CC analysis of the  $(\alpha, \alpha')$  data for the Hoyle state are shown in Fig. 3. The effects of the higher-order coupling effects are best seen in the 240 MeV results. The DWBA1 calculation using the (rescaled) AMD transition density would give the best-fit  $M(E0 \uparrow) \approx 3.65 e \text{ fm}^2$ . The CC calculation including all possible transitions from the Hoyle state to the neighboring cluster states (see Fig. 2) gives  $M(E0 \uparrow) \approx 4.5 e \text{ fm}^2$ , which is about 20% stronger than that given by the standard DWBA analysis. It is expected that a full coupled reaction channel analysis of the  $(\alpha, \alpha')$  data including also breakup channels would yield the best-fit  $M(E0 \uparrow)$  value closer to the  $(e, e')$  data. That would physically explain the missing monopole strength of the Hoyle state in  $(\alpha, \alpha')$

scattering that can be accounted for in the DWBA only by an enhanced absorption in the exit channel [16].

The MDA of the  $(\alpha, \alpha')$  data measured at  $E_\alpha = 386$  MeV has shown a broad  $0_3^+$  resonance and a narrow  $2_2^+$  state centered at the excitation energies  $E_x \approx 9.93$  and 9.84 MeV, respectively. After the subtraction of the known  $0_2^+$ ,  $3_1^-$ , and  $1_1^-$  peaks, the total  $(\alpha, \alpha')$  angular distribution deduced for the wide bump centered at  $E_x \approx 10$  MeV has been shown [10] to contain only the coherent contributions from the  $2_2^+$  and  $0_3^+$  states (see Fig. 4). Given the  $E0$  strength of the  $0_3^+$  state accurately determined in the analysis of the 240 MeV data [13], the  $E2$  strength of the  $2_2^+$  state remains the only parameter in the present CC analysis of the 386 MeV  $(\alpha, \alpha')$  data. Although the  $\alpha$  energy of 386 MeV can be considered as high enough for the validity of the DWBA, very strong  $E\lambda$  transitions between the  $2_2^+$  state and other cluster states of  $^{12}\text{C}$  lead to quite the significant CC effect. We found that the calculated  $(\alpha, \alpha')$  cross section for the  $2_2^+$  state is indeed enhanced by the indirect excitation of the  $2_2^+$  state via other excited states. As a result, the best CC description of the  $(\alpha, \alpha')$  cross section for the  $2_2^+$  and  $0_3^+$  states was obtained with the  $2_2^+$  transition density rescaled to give  $B(E2; 0_1^+ \rightarrow 2_2^+) \approx 3 e^2 \text{ fm}^4$ , about 50% larger than that predicted by the AMD calculation. This result is in a fine agreement with  $B(E2 \uparrow) \approx 3.65 e^2 \text{ fm}^4$  given by the analysis of the photodissociation data [11].

A natural question now is why the  $2_2^+$  state was not observed at  $E_x \approx 10$  MeV in the  $(\alpha, \alpha')$  experiment at  $E_\alpha = 240$  MeV. Given the realistic  $E\lambda$  strengths of the isoscalar states found in our folding model + CC analysis of the both data sets, we have considered explicitly the contributions of the different multipole strengths in the energy bins around 10 MeV on the 240 MeV data [14]. The  $E\lambda$  transition strengths of the  $2_2^+$ ,  $0_3^+$  and  $1_1^-$  states were distributed over the corresponding widths determined from the experiment. The CC description of the 240 MeV  $(\alpha, \alpha')$  data measured for the energy bins closest to  $E_x = 10$  MeV is shown in Fig. 5. From the calculated total cross section with and without the contribution from the  $2_2^+$  state one can see clearly that the  $E2$  strength of the  $2_2^+$  state is indeed present in these energy bins. Because the CC description of the  $(\alpha, \alpha')$  data shown in Fig. 5 has been obtained without any further readjusting the  $E\lambda$  strengths of the involved cluster states, we conclude that the presence of the  $2_2^+$  state at the energy near 10 MeV has been found in the  $(\alpha, \alpha')$  spectrum measured at  $E_\alpha = 240$  MeV. Such a subtle effect could not be resolved in the original MDA of these data [14].

The  $(\alpha, \alpha')$  data at  $E_\alpha = 386$  MeV was measured using the high-precision Grand Raiden spectrometer, and the  $(\alpha, \alpha')$  spectrum over the whole energy and angular range has been obtained free of background [10]. At variance with the MDA of the 240 MeV data, the MDA of the 386 MeV data has revealed a clear presence of the  $2_2^+$  state at  $E_x \approx 10$  MeV, and the total  $(\alpha, \alpha')$  cross section measured at this energy was used above in our analysis to determine the realistic  $E2$  strength of the  $2_2^+$  state (see Fig. 4). Given the 386 MeV data available for the energy bins around

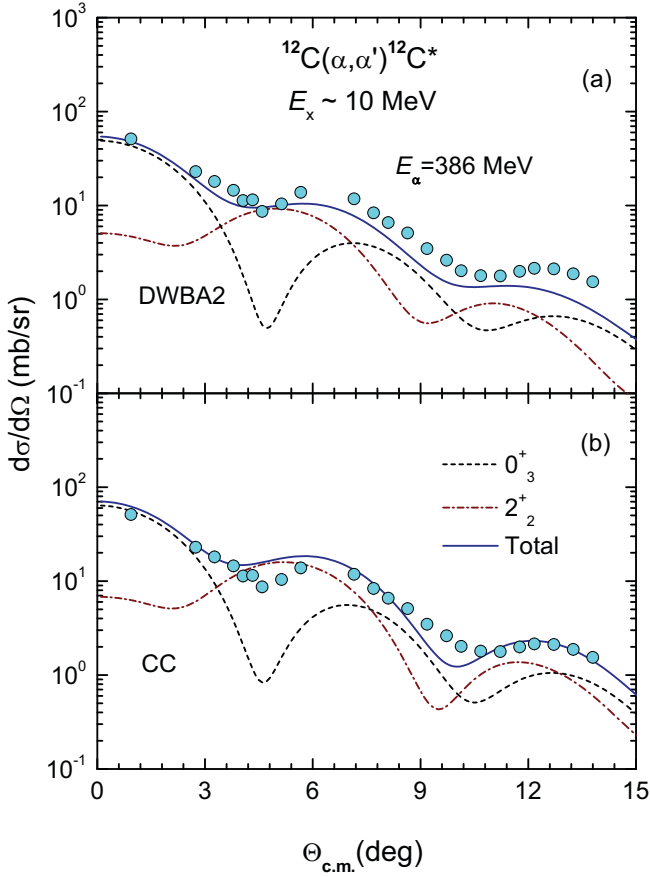


**Figure 4.** (Color online) DWBA (a) and CC (b) descriptions of the  $(\alpha, \alpha')$  data measured at  $E_\alpha = 386$  MeV for the  $0_3^+$  and  $2_2^+$  states [10]. The DWBA2 and CC results were obtained in the same way as described in the caption of Fig. 3. The AMD transition density of the  $2_2^+$  state has been rescaled to the best CC fit to the data, giving  $B(E2; 0_1^+ \rightarrow 2_2^+) \approx 3 e^2 \text{fm}^4$ .

$E_x = 10$  MeV, it is complimentary to probe the consistency of the present folding model + CC approach in the analysis of the  $(\alpha, \alpha')$  data at  $E_\alpha = 386$  MeV, similar to that shown in Fig. 5. All the remaining inputs of the folding model + CC calculation were determined in the same manner as that done above for the 240 MeV data. The CC description of the 386 MeV  $(\alpha, \alpha')$  data measured for the three energy bins around  $E_x \approx 10$  MeV is shown in Fig. 6. One can see that a good overall agreement of our CC results with the  $(\alpha, \alpha')$  data measured at  $E_\alpha = 386$  MeV for these energy bins is obtained with the same structure inputs for the important cluster states of  $^{12}\text{C}$  as those used to obtain the CC results at 240 MeV. The CC results for the three energy bins obtained with the  $E2$  strength of the  $2_2^+$  state distributed over the total width  $\Gamma = 2.1$  MeV are shown in Fig. 6, and one can see a good agreement of the CC results with the data, especially, a very good CC description of the data at the energy bin centered at  $E_x = 10.125$  MeV. Thus, the CC results shown in Figs. 5 and 6 consistently confirm that total width of the  $2_2^+$  state should be around 2 MeV as determined from the photodissociation data [12].

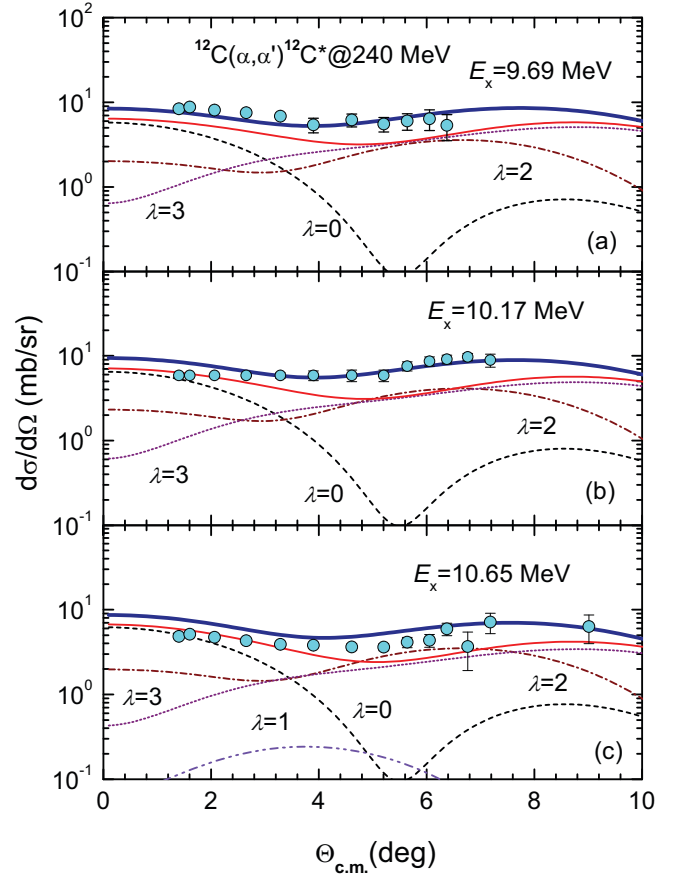


**Figure 5.** (Color online) Differential  $(\alpha, \alpha')$  cross sections measured at  $E_\alpha = 240$  MeV [14] for the 475 keV-wide energy bins centered at  $E_x = 9.69$  MeV (a), 10.17 MeV (b), and 10.65 MeV (c), and the CC results given by the different multipole transition strengths. The total cross sections obtained with and without the contribution from the  $2_2^+$  state are shown as the thick (blue) and thin (red) solid lines, respectively. The  $E2$  strength of the  $2_2^+$  state is distributed over the width  $\Gamma = 2.1$  MeV as determined from the photodissociation experiment [12].

In conclusion, the complex OP and inelastic FF obtained from the folding model using the nuclear transition densities predicted by the AMD approach [7] and the density dependent CDM3Y6 interaction [18] have been used in a comprehensive CC calculation of the  $(\alpha, \alpha')$  data measured at  $E_\alpha = 240$  and 386 MeV. The detailed folding model + CC analysis of the  $(\alpha, \alpha')$  data measured in the energy bins around  $E_x \approx 10$  MeV has revealed clearly the  $E2$  transition strength that should be assigned to the  $2_2^+$  state of  $^{12}\text{C}$ . The presence of the  $2_2^+$  state of  $^{12}\text{C}$  has been consistently confirmed in the CC analysis of the both 240 and 386 MeV data sets.

Given the strong  $E\lambda$  strengths predicted for the transitions between the  $2_2^+$  state and other cluster states of  $^{12}\text{C}$ , the high-precision  $(\alpha, \alpha')$  measurement at the lower incident energies should be the interesting alternative experiment to observe the  $2_2^+$  excitation and probe the indirect (two-step) excitation of this state via the CC scheme shown in Fig. 2.



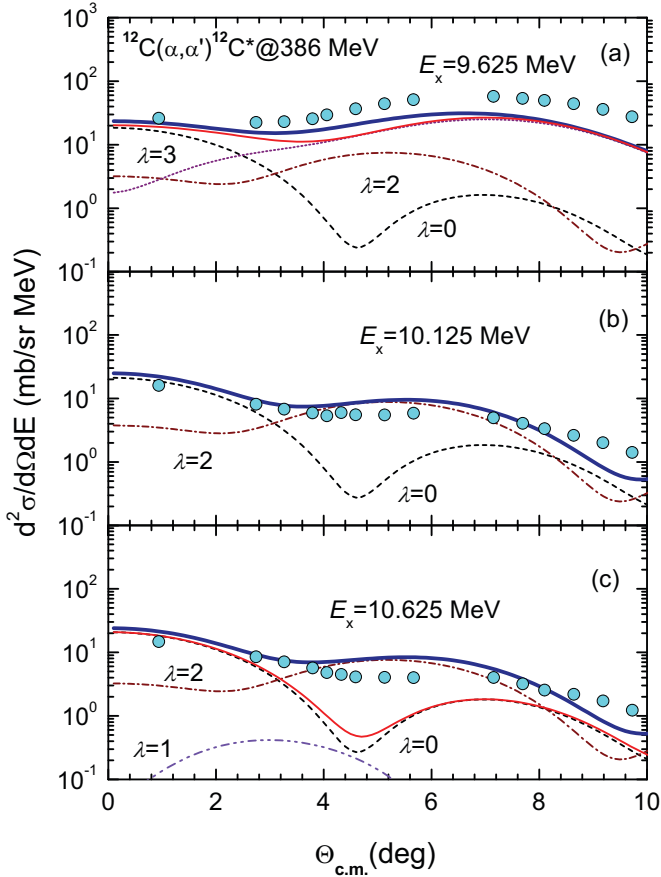


**Figure 6.** (Color online) Double-differential ( $\alpha, \alpha'$ ) cross sections measured at  $E_\alpha = 386$  MeV [10] for the 250 keV-wide energy bins centered at  $E_x = 9.625$  MeV (a), 10.125 MeV (b), and 10.625 MeV (c), in comparison with the CC results in the same way as in Fig. 5.

The results of the present study have shown clearly why the  $2_2^+$  state of  $^{12}\text{C}$  has been so hard to find, taking over 50 years in its discovery. The puzzle with the excitation of the Hoyle state seems now to be finally understood.

## Acknowledgements

We thank Martin Freer, William Zimmerman, and the authors of Refs. [10, 14] for the helpful communications. The present research has been supported, in part, by the National Foundation

for Science and Technology Development (NAFOSTED) under Project No. 103.04-2014.76.

## References

- [1] F. Hoyle, *Astrophys. J. (Supplement Series)* **1**, 12 (1954)
- [2] C.W. Cook, W.A. Fowler, C.C. Lauritsen, and T. Lane, *Phys. Rev.* **107**, 508 (1957)
- [3] M. Freer and H. Fynbo, *Prog. Part. Nucl. Phys.* **78**, 1 (2014)
- [4] H. Morinaga, *Phys. Rev.* **101**, 254 (1956)
- [5] E. Uegaki, S. Okabe, Y. Abe, and H. Tanaka, *Prog. Theor. Phys.* **57**, 1262 (1977)
- [6] M. Kamimura, *Nucl. Phys. A* **351**, 456 (1981)
- [7] Y. Kanada-En'yo, *Prog. Theor. Phys.* **117**, 655 (2007)
- [8] D.T. Khoa, D.C. Cuong and Y. Kanada-En'yo, *Phys. Lett. B* **695**, 469 (2011)
- [9] M. Freer *et al.*, *Phys. Rev. C* **86**, 034320 (2012)
- [10] M. Itoh *et al.*, *Phys. Rev. C* **84**, 054308 (2011)
- [11] W.R. Zimmerman *et al.*, *Phys. Rev. Lett.* **110**, 152502 (2013)
- [12] W.R. Zimmerman, PhD Dissertation, University of Connecticut (2013)
- [13] D.C. Cuong, D.T. Khoa, and Y. Kanada-En'yo, *Phys. Rev. C* **88**, 064317 (2013)
- [14] B. John, Y. Tokimoto, Y.W. Lui, H.L. Clark, X. Chen, and D.H. Youngblood, *Phys. Rev. C* **68**, 014305 (2003)
- [15] P. Strehl, *Z. Phys.* **234**, 416 (1970)
- [16] D.T. Khoa and D.C. Cuong, *Phys. Lett. B* **660**, 331 (2008)
- [17] D.T. Khoa and G.R. Satchler, *Nucl. Phys. A* **668**, 3 (2000)
- [18] D.T. Khoa, G.R. Satchler, and W. von Oertzen, *Phys. Rev. C* **56**, 954 (1997)
- [19] D.C. Cuong, D.T. Khoa, and G. Colò, *Nucl. Phys. A* **836**, 11 (2010)
- [20] J.P. Jeukenne, A. Lejeune, and C. Mahaux, *Phys. Rev. C* **16**, 80 (1977)
- [21] J. Raynal, *Computing as a Language of Physics* (IAEA, Vienna, 1972) 75; J. Raynal, coupled-channel code ECIS97 (unpublished)